

AMCoR

Asahikawa Medical University Repository <http://amcor.asahikawa-med.ac.jp/>

Journal of Applied Physics (2010) 108(8):084301-1-6.

Broad energy-bands of continuous-network-structure molybdenum films

Anno, Eiji

Broad energy-bands of continuous-network-structure molybdenum films

Eiji Anno^{a1}*Department of Physics, Asahikawa Medical College, Asahikawa, Hokkaido 078-8510, Japan*

(Received 26 April 2010; accepted 31 August 2010; published online 18 October 2010)

Interband absorption of continuous-network-structure (CNS) molybdenum films with a weight thickness below about 3 nm weakened and shifted to higher energies compared to interband absorption of continuous-thin molybdenum films with bulk energy bands. This weakening and shift agrees qualitatively with that observed in interband absorption of metal particles, which have energy bands broadened by lattice contraction. Based on this agreement, the weakening and shift in the CNS molybdenum films can be qualitatively ascribed to energy-band broadening. Thus, CNS molybdenum films with a weight thickness below about 3 nm have broader energy bands compared to bulk molybdenum. © 2010 American Institute of Physics. [doi:10.1063/1.3496682]

I. INTRODUCTION

Energy bands of metals are of fundamental interest in solid state physics. Interband absorption, due to transitions between electronic states in energy bands, reflects the energy band structure. Thus, the investigation of interband absorption of metals is useful for an understanding of the energy bands of metals.

The formation of a continuous-thin metal film on an amorphous substrate by vacuum evaporation involves the following steps:¹ (1) formation of small nuclei; (2) growth of the nuclei into island particles; (3) growth of the island particles by the coalescence of smaller island particles; (4) formation of a continuous-network-structure (CNS) film by the coalescence of large island particles; and (5) a continuous-thin film. Island particles will hereafter be referred to as "particles."

A system consisting of particles distributed on the substrate surface is called the island film. CNS metal films, in which the metal deposit is separated by long, irregular, and narrow channels, are intermediate between continuous-thin metal films and metal-island films. Interband absorption of continuous-thin metal films is almost the same as that of the bulk metal,² and thus showing energy bands almost the same as those of the bulk metal. Lattice constants of metal particles contract with decreasing particle size because of the hydrostatic pressure due to the particle surface stress.³ Studies of interband absorption of metal-island films⁴⁻⁶ have shown that energy bands of metal particles broaden with lattice contraction.

There has been very little study of interband absorption and energy bands of CNS metal films. If the interband absorption of CNS metal films is different from that of bulk metal, by analyzing the difference, we can understand the characteristics of the energy bands of CNS metal films.

Molybdenum, a body-centered-cubic (bcc) transition metal, was chosen in the present study because this metal tended to form CNS films. The interband absorption of CNS molybdenum films is compared to that of continuous-thin molybdenum films, which is almost the same as that of bulk

molybdenum. Based on the difference in strength and location of the interband absorption between these films, the energy bands of CNS molybdenum films are discussed qualitatively.

II. EXPERIMENT

Samples used in the present study were continuous-thin molybdenum films and CNS molybdenum films.

In a vacuum chamber, a fused-quartz substrate ($18 \times 18 \times 0.5$ mm³) and transmission electron-microscope meshes covered with a carbon film were placed adjacently above an evaporation source. The distance from the evaporation source to the substrate and meshes was 30.3 cm. SiO₂ was first deposited both on the substrate and meshes by electron-beam heating in an oil-free vacuum of $\sim 10^{-8}$ Torr. Next, at pressures of $\sim 10^{-7}$ Torr, molybdenum (purity 99.9%) was deposited to obtain continuous-thin films or CNS films. The films were then annealed for 1 h. During deposition and annealing, the substrate and meshes were maintained at a temperature of about 773 K. After annealing, to prevent adsorption or chemical reactions on exposure to air, the films were coated with SiO₂ (thickness 10–30 nm). The weight thickness (nanometer), which corresponds to the effective thickness for an ideal continuous film with bulk density, and the deposition rate (nanometer per second) were monitored with a quartz-crystal oscillator.

Optical and electron-microscopic investigations were carried out after exposing the samples to air. With a double-beam spectrophotometer (Shimadzu UV-365), transmittance spectra for normal incidence and their first derivatives were measured in the wavelength range of 190–2500 nm at room temperature within an experimental accuracy of $\pm 0.1\%$ and $\pm [0.3 (190 \text{ nm}) - 0.7 (2500 \text{ nm})]$ nm. The first-derivative spectra were derived by computer applications based on the convolution method for a wavelength interval of about 4 nm. The image and electron-diffraction pattern of the films were investigated with electron microscopes operating at 200 kV (Hitachi H-800) [Figs. 1(a) and 2] and 100 kV (JEOL JEM-1010) [Figs. 1(b)-1(c')].

^{a1}Electronic mail: anno@asahikawa-med.ac.jp.

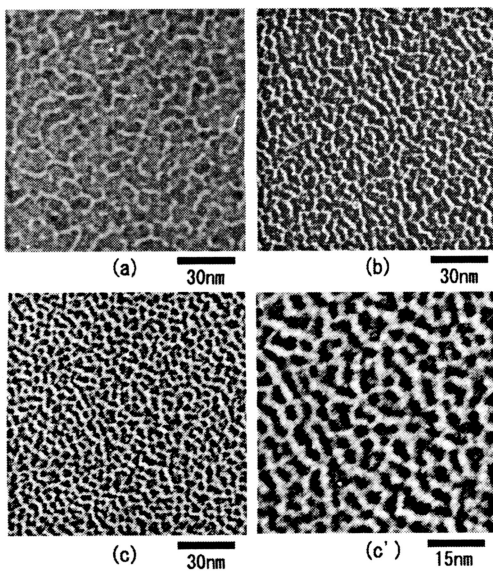


FIG. 1. Electron micrographs for CNS molybdenum films with weight thicknesses of (a) 3.03, (b) 2.27, and (c) 1.52 nm. (c') is the twice enlarged relative to (c). The optical spectra of films (a), (b), and (c) are shown in Figs. 3(b)–3(d), respectively.

III. RESULTS

A. Electron-microscopic investigation

In the present study, CNS films were formed when the weight thickness was below about 5 nm. Figures 1(a)–1(c) show the bright field images of CNS molybdenum films with weight thicknesses of 3.03 nm, 2.27 nm, and 1.52 nm, respectively. The magnification of the micrographs is identical ($\times 320\,000$). Long, irregular, and narrow channels, which are characteristic of CNS films, are observed in these figures. Figure 1(c') is twice enlarged with respect to Fig. 1(c). It is seen in Fig. 1(c') that the molybdenum deposit is connected by thin molybdenum lines in places.

CNS metal films are usually polycrystalline.¹ CNS gold,¹ silver,⁷ and iridium films,⁷ for example, are known to be polycrystalline. The contrast of the film of Fig. 1(a) is not uniform because of the diffraction contrast, showing the film

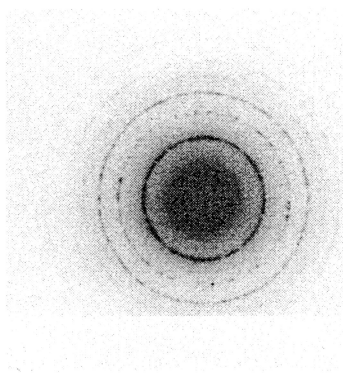


FIG. 2. The electron-diffraction pattern of a continuous-thin molybdenum film with a weight thickness of 6.82 nm. The optical spectra of this film are shown in Fig. 3(a).

to be in a polycrystalline state.⁸ The films in Figs. 1(b) and 1(c) are presumably also in polycrystalline states, although not uniform contrast, as shown in Fig. 1(a), was difficult to investigate for these films.

Figure 2 shows the electron-diffraction pattern of the continuous-thin molybdenum film with a weight thickness of 6.82 nm. The pattern consists of the rings, evidence that the film is polycrystalline. This pattern represents the bcc structure, e.g., the smallest and thick ring corresponds to (110) and the next ring corresponds to (200).

In the present study, only the bcc structure, such as shown in Fig. 2, could always be identified in electron-diffraction patterns of the films with a weight thickness above about 3 nm [Fig. 1(a)]. This implies that compound layers, such as molybdenum oxide layer, are formed rarely on the film surface, or that the films change rarely into compound. When the weight thickness is below about 3 nm, the electron-diffraction patterns of CNS films [Figs. 1(b) and 1(c)] were difficult to observe because of the low contrast. Thus, the crystal structure of these films could not be identified. Particles of chromium (a bcc transition metal) have been known to have A-15 type structure.⁹ If molybdenum films had such a structure, the optical absorption would be entirely different from that of molybdenum films with a bcc structure. As shown below (Fig. 3) (Sec. III B), interband absorption with peak at about 4.3 eV, the intrinsic absorption of molybdenum, was found down to the thinnest weight thickness (0.76 nm) [Fig. 3(c)] in the present study. Based on this, CNS molybdenum films with a weight thickness below about 3 nm were regarded to have a bcc structure.

The contraction of lattice constants was investigated for the diameters of the (110) and (200) electron-diffraction rings. There was little difference in diameter between films with a weight thickness above about 3 nm [Fig. 1(a)], showing no change in the lattice constants. If lattice constants contracted, this would have been observed in films with a weight thickness below about 3 nm.

B. Spectra of CNS molybdenum films

In the following figures, to show experimental spectra compactly, the wavelength unit (nanometer) (Sec. II) is converted into the photon energy unit (electron volt). Due to the conversion, the slope sign of the derivative is reverse.

In derivative spectroscopy,¹⁰ the location of the maximum slope in a step appearing in the first derivative corresponds to that of absorption. In the following figures, the arrow indicates the location of the maximum slope in the step, and in the transmittance spectrum, this location is labeled with a number as the location of absorption. In the present paper, the location of absorption is expressed by $E \pm \Delta E$, shows that the slope is at its maximum in the range of $(E - \Delta E) - (E + \Delta E)$. When the slope in the step is monotonous, the location of the maximum slope is difficult to identify. In that case, the range of the location (i.e., the range of the monotonous slope) is represented by a double-ended horizontal arrow.

There are several differences between previously reported data on the optical spectrum of molybdenum.^{2,11–13}

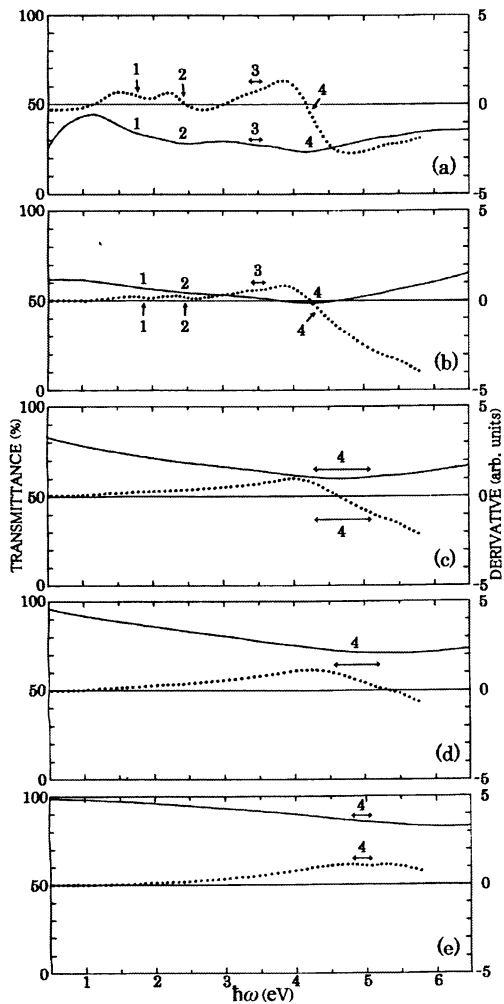


FIG. 3. Transmittance spectra (solid curves) and first derivatives (dotted curves) of CNS molybdenum films with weight thicknesses of (a) 6.82, (b) 3.03, (c) 2.27, (d) 1.52, and (e) 0.76 nm. The deposition rate was 0.006 nm/s.

The dielectric constant spectrum of the vacuum-evaporated films (polycrystalline) of Ref. 2 is similar to that of the bulk (single crystal) of Refs. 11,¹³ though these spectra show small discrepancies in the absolute values of the dielectric constants.¹³ Samples in the present study are vacuum-evaporated films (polycrystalline) (Sec. III A). Thus, in this study, the data in Ref. 2 is considered to be the most relevant reference data.

Transmittance of the evaporated SiO₂ film was almost constant within the spectral range of interest here because absorption of the evaporated SiO₂ film, which is thin (Sec. II), was weak in the range above about 5 eV.

Figure 3(a) shows the transmittance spectrum and its derivative for the continuous-thin molybdenum film with a weight thickness of 6.82 nm, the thickest in the present study. Absorption in Fig. 3(a) is almost in agreement with that of Ref. 2 (i.e., the reference data): absorption below about 1 eV is the overlap¹³ of interband absorption and Drude-type absorption, due to conduction electrons and in-

creases with decreasing energy, and absorption 1–4, located at 1.77 ± 0.07 eV, 2.42 ± 0.05 eV, $3.35\text{--}3.56$ eV, and 4.25 ± 0.05 eV, respectively, are interband absorption.¹³ The almost agreement shows the film in Fig. 3(a) to have energy bands almost the same as those of bulk molybdenum. In the following, absorption 1–4 is referred to as interband absorption 1–4, respectively.

In Fig. 3(a), a very weak dip is present at about 5.5 eV in the transmittance spectrum. This dip was difficult to investigate because the step for the dip is ill defined in the derivative (possibly the structure in the range of about 5.2–5.6 eV). The cause of the very weak dip could not be made clear in the present study. This dip was not found in the films with a weight thickness below that in Fig. 3(a) (6.82 nm).

By comparing the interband absorption of CNS molybdenum films with that in Fig. 3(a) (i.e., the reference data), we can investigate the difference in energy bands between the CNS molybdenum films and bulk molybdenum.

When a metal-island film consists of metal particles smaller than the wavelength of the incident light, the absorption due to conduction electrons is not Drude-type absorption but optical plasma-resonance absorption caused by plasma oscillations of conduction electrons in the metal particles.¹⁴

For CNS silver and iridium films,⁷ it has been shown that the region that is mostly surrounded by channels is a particlelike region where the conduction electrons behave as in a metal particle, and that absorption due to conduction electrons in the particlelike region is optical plasma-resonance absorption.

From this, Drude-type absorption is predicted not to occur in CNS molybdenum films composed almost of particlelike regions.

The transmittance spectrum and its derivative for the CNS molybdenum film with a weight thickness of 3.03 nm are shown in Fig. 3(b). The locations of interband absorption 1–4 are 1.84 ± 0.07 eV, 2.44 ± 0.07 eV, $3.39\text{--}3.61$ eV, and 4.34 ± 0.08 eV, respectively. Drude-type absorption, shown in Fig. 3(a), is not found below about 1 eV, so that this CNS film is composed almost of particlelike regions. Optical plasma-resonance absorption of the particlelike regions, not found in the spectra in Fig. 3(b), is presumably present above about 6.5 eV.

In Fig. 3(b), the almost constant transmittance in the range of about 0.5–1 eV reveals the interband absorption of molybdenum separated from Drude-type absorption. Such separated interband-absorption has also been found for island films of vanadium¹⁵ (a bcc transition metal), in which Drude-type absorption does not occur as described above. The appearance of the separated interband-absorption in the vanadium-island films and the CNS molybdenum film in Fig. 3(b) supports that this CNS molybdenum film is composed almost of particlelike regions.

The other CNS molybdenum films in Figs. 3(c)–3(e), for which, as in the case of the film in Fig. 3(b), Drude-type absorption and optical plasma-resonance absorption are not found, also almost consist of particlelike regions.

It has not been reported that particlelike regions influence interband absorption. Thus, particlelike regions are not taken into account in the following consideration of interband absorption.

Interband absorption 1–4 in Fig. 3(a) (i.e., in the reference data) occurs in the CNS molybdenum film in Fig. 3(b). Thus, this CNS molybdenum film has energy bands almost the same as those of bulk molybdenum.

Based on an experimental study, Ref. 12 pointed out that in addition to interband absorption 1–4 interband absorption is present at about 1.35, 2.70, 3.30, and 4.60 eV. References 2 and 11 have not reported such the interband absorption. In the present study, as shown in Figs. 3(a) and 3(b), interband absorption was not detected at these locations. This seems to be because the interband absorption pointed out by Ref. 12 is weak compared to interband absorption 1–4.

The increase in the transmittance with increasing energy above about 5.5 eV is gentler in Fig. 3(a) than in Fig. 3(b). The reason for this difference is not clear.

The transmittance spectra and the derivatives for the CNS molybdenum films with weight thicknesses of 2.27 nm and 1.52 nm are shown in Figs. 3(c) and 3(d), respectively. In contrast to Fig. 3(b), the transmittance is not constant in the range of about 0.5–1 eV, indicating the change in interband absorption. The steps for interband absorption 1–3, found in Fig. 3(b), were not detected by the derivatives. This shows that interband absorption 1–3 weakens when the weight thickness is below about 3 nm [Fig. 3(b)].

The location of interband absorption 4 was difficult to identify in Figs. 3(c) and 3(d), in which the range of the location is 4.28–5.10 eV and 4.55–5.22 eV, respectively, showing that the step in the derivative is ill-defined compared to Fig. 3(b) because, as for interband absorption 1–3, this absorption weakens. Thus, interband absorption 4 also weakens when the weight thickness is below about 3 nm.

Figure 3(e) shows the transmittance spectrum and its derivative for the molybdenum film with a weight thickness of 0.76 nm. This film was difficult to observe by electron microscope because of the low contrast. The spectra of Fig. 3(e) are similar to those of Figs. 3(c) and 3(d): the transmittance is not constant in the range of about 0.5–1 eV, the steps for interband absorption 1–3 are not detected by the derivative, and interband absorption 4, located in the range 4.78–5.08 eV, is weaker than that in Fig. 3(b). Based on these similarities, the film in Fig. 3(e) was regarded to be a CNS film.

Compared to Figs. 3(c) and 3(d), interband absorption 4 in Fig. 3(e) is appreciably weak. This shows that interband absorption 4 weakens with decreasing weight thickness below about 3 nm.

In the transmittance spectra of Figs. 3(d) and 3(e), we see that absorption is present above about 5.5 eV. The absorption should be present in the spectra of Figs. 3(a)–3(c) as well. The structure located at about 5.5 eV in the derivatives of Figs. 3(b)–3(d) and the structure located at about 5 eV in the derivative of Fig. 3(c) are due to the overlap of interband absorption 4 and absorption in the range above about 5.5 eV. The structure due to the overlap is difficult to find in the derivative of Fig. 3(a). This may be because the structure is contained in the ill defined step (possibly in the range of

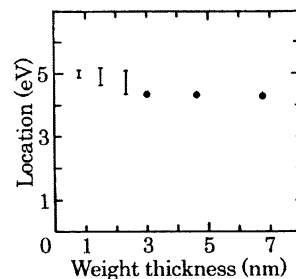


FIG. 4. The locations of interband absorption 4 vs the weight thickness. The bars correspond to the double-ended horizontal arrows in Figs. 3(c)–3(e).

about 5.2–5.6 eV) mentioned above. Absorption above about 5.5 eV was difficult to investigate because the step in the derivative was incomplete.

C. Location of interband absorption 4

Figure 4 plots the location of interband absorption 4 against weight thickness. The location for the CNS molybdenum film with a weight thickness of 4.55 nm is plotted as well, though the spectra are not given in the present paper. The locations of interband absorption 1–4 for this CNS film are 1.77 ± 0.10 eV, 2.43 ± 0.05 eV, 3.31 – 3.60 eV, and 4.26 ± 0.10 eV, respectively.

We see in Fig. 4 that when the weight thickness is below about 3 nm interband absorption 4 shifts to higher energies.

If the energy bands of continuous-thin molybdenum films and CNS molybdenum films are almost the same as those of bulk molybdenum, the location of interband absorption must be irrespective of weight thickness. In Fig. 4, the locations are almost constant for the weight thickness above about 3 nm. The locations of interband absorption 1–3 of the films with a weight thickness of 3.03, 4.55, and 6.82 nm, mentioned above, are also almost constant. Therefore, the continuous-thin molybdenum films and CNS molybdenum films with a weight thickness above about 3 nm have energy bands almost the same as those of bulk molybdenum. This agrees with the bulk energy bands of the films of Fig. 3(a) (weight thickness: 6.82 nm) and Fig. 3(b) (weight thickness: 3.03 nm) mentioned in Sec. III B.

IV. DISCUSSION

A. Transitions for interband absorption 1–4

Interband absorption of molybdenum has been studied by several authors.^{2,11–13} In these studies, considerable effort has been devoted to identify transitions for interband absorption, however, the proposed transitions are different, as mentioned below.

E_F denotes the Fermi energy. Based on measurements on single crystals, Weaver *et al.*¹¹ have attributed interband absorption 1, 2, and 4 to the transitions $\Delta_5(E_F) \rightarrow \Delta'_2$, $\Sigma_1 \rightarrow \Sigma_1$, and $G_1 \rightarrow G_1$, respectively. Nestell and Christy² have measured vacuum-evaporated films (polycrystalline). They assigned interband absorption 4 to the transition $\Lambda_3 \rightarrow \Lambda_3$. Colavita *et al.*¹² have measured single crystals and ascribed interband absorption 1–4 to the transitions $\Sigma_1(E_F) \rightarrow \Sigma_1$, $\Sigma_1(E_F) \rightarrow \Sigma_4$, $\Delta_5(E_F) \rightarrow \Delta_1$, and $\Delta_5(E_F) \rightarrow \Delta_1$, respectively.

Romaniello *et al.*¹³ have theoretically related interband absorption 1 and 2, 3, and 4 to the transitions between the Fermi level of band 3 and band 4 in the region of Γ HN plane, the transition $N'_1(E_F) \rightarrow N_4$, and the transition $\Delta_5(E_F) \rightarrow \Delta_1$, respectively.

Although transitions for interband absorption 1–4 have not been identified as yet, the abovementioned studies reveal that interband absorption 1–4 is due to direct transitions between the initial states (the occupied states) at or below the Fermi level and the final states (the empty states) above the Fermi level.

B. Broad energy-bands

When the weight thickness is below about 3 nm, interband absorption 1–4 weakens (Sec. III B), and interband absorption 4 shifts to higher energies (Sec. III C). This shift is not observed in interband absorption 1–3 (Fig. 3). Nevertheless, a slight shift, even though not visible in the spectra, is expected to occur because interband absorption 1–3 and interband absorption 4 are similar in that both weaken below about 3 nm.

In direct transition, the weakening and shift mentioned above are, respectively, due to the decrease in the joint density of states (JDOS) and the increase in energy spacing between the initial and the final states.¹⁶ Thus, both the decrease in JDOS and the increase in energy spacing must occur when the weight thickness is below about 3 nm.

As is well known, when energy bands of metals broaden, the density of states (DOS) decreases, which is generally attended with an decrease in JDOS,¹⁷ and the energy spacing between the occupied and empty states increases.¹⁷ Thus, the energy-band broadening causes the interband absorption to both weaken and shift to higher energies.

As mentioned in Sec. I, lattice contractions occur in metal particles.³ It has been accepted that energy bands broaden with lattice contraction.¹⁸ Energy-band broadening due to lattice contraction has been reported for copper,^{4,5} gold,⁵ and ruthenium particles.⁶ In the reports,^{4–6} it has been shown that when energy bands broaden, interband absorption of metal particles weakens and shifts to higher energies. This weakening and shift agrees qualitatively with that observed in CNS molybdenum films with a weight thickness below about 3 nm.

There is very little data on the energy-band broadening of molybdenum. Here, I refer to a theoretical study of the energy-band broadening of vanadium.¹⁹ Vanadium and molybdenum are bcc transition metals and adjacent in the periodic table, and thus their band dispersions are similar, i.e., the energy bands of these metals resemble each other. Using the augmented-plane-wave method, Papaconstantopoulos *et al.*¹⁹ have calculated the energy bands of vanadium self-consistently for normal and 5%-reduced lattice constants. The calculated energy bands for the reduced lattice constant show energy-band broadening compared to the normal lattice constant the DOS decreases (e.g., the decrease at the Fermi level is about 20%) and the energy spacing between the occupied and empty states increases (e.g., the increase in the energy spacing between G_1 and G_1 is about 30%). Similar

changes in the DOS and energy spacing presumably occur also in the energy-band broadening of molybdenum.

At present, energy-band broadening is the only factor widely accepted to cause both a decrease in the JDOS and an increase in energy spacing between the occupied and empty states.

From this discussion, the weakening and shift to higher energies of the interband absorption of CNS molybdenum films with a weight thickness below about 3 nm can be qualitatively ascribed to energy-band broadening. Therefore, CNS molybdenum films have broader energy bands compared to bulk molybdenum.

The weakening of interband absorption 1–3 with a slight shift mentioned above is presumably because the JDOS for interband absorption 1–3 decreases early in the energy-band broadening.

The weakening and shift in interband absorption 1–4 were difficult to discuss quantitatively because very little data on the energy-band broadening of molybdenum has been reported to date.

The energy bands for a bcc structure can be broadened only by lattice contraction. Thus, the energy-band broadening for CNS molybdenum films with a weight thickness below about 3 nm is thought to be due to lattice contraction.

The film in Fig. 3(e) was difficult to observe by electron microscope (Sec. III B). This film may be an island film consisting of molybdenum particles. In the case of an island film, the weakening and shift to higher energies of interband absorption 1–4 of molybdenum particles [Figs. 3(c) and 4] are similar to those of metal particles^{4–6} having energy bands broadened by lattice contraction. The similarity shows that the molybdenum particles have energy bands that are broader than those of bulk molybdenum. The weakening and shift to higher energies of interband absorption 1–4 of the CNS molybdenum films [Figs. 3(c), 3(d), and 4] agree qualitatively with those of molybdenum and the metal particles.^{4–6} This shows that the energy bands of the CNS molybdenum films broaden as in the case of molybdenum and the metal particles. Therefore, even if the film of Fig. 3(e) is an island film, the CNS molybdenum films in Figs. 3(c) and 3(d) can be shown to have energy bands broader than those of bulk molybdenum.

Very little has been studied about the interaction between the SiO₂ matrix and molybdenum. As in a previous paper,¹⁵ the interaction will be considered below from the viewpoint of the final-state occupation.

If electrons of the SiO₂ matrix occupy the final states for transitions for interband absorption 1–4, the transitions would be restricted and thus interband absorption 1–4 would weaken as in Fig. 3. There is very little data on E_F of CNS molybdenum films. E_F is assumed here to be the same as that of bulk molybdenum, and as in the case by Ashcroft and Mermin,²⁰ E_F was calculated from the lowest valence (3) (Ref. 21) and the lattice constant (0.315 nm) (Ref. 22) of bulk molybdenum. E_F of CNS molybdenum films is about 6.5 eV higher than that of bulk silver, and E_F of bulk silver is about 6.3 eV higher than the valence-band maximum of SiO₂.²³ From these values, E_F of CNS molybdenum films is much higher (about 12.8 eV) than the valence-band maxi-

num of SiO_2 . Thus, the valence band of SiO_2 does not overlap the final states lying at values higher than E_F , i.e., the electrons of the SiO_2 matrix cannot occupy the final states. Therefore, the weakening of interband absorption 1–4 is not due to the occupation of the final states.

V. SUMMARY

Energy bands of CNS molybdenum films were studied qualitatively by comparing the interband absorption of CNS molybdenum films with that of continuous-thin molybdenum films having bulk energy bands. Interband absorption of CNS molybdenum films with a weight thickness below about 3 nm weakened and shifted to higher energies compared to the interband absorption of the continuous-thin molybdenum film. Referring to the interband absorption of metal particles having energy bands broadened by lattice contractions, the weakening and shift can be qualitatively attributed to energy-band broadening. Thus, the energy bands of CNS molybdenum films with a weight thickness below about 3 nm are broader than those of bulk molybdenum.

ACKNOWLEDGMENTS

I am grateful to Professor Masayuki Ido (Hokkaido University) for his encouragement throughout this work. I also thank Dr. Tomuo Yamaguchi for informative discussions.

¹See, for example, D. W. Pashley, M. J. Stowell, M. H. Jacobs, and T. J. Low, *Philos. Mag.* **10**, 127 (1964); D. W. Pashley, *Adv. Phys.* **14**, 327 (1965), and references therein.

²See, for example, J. E. Nestell, Jr. and R. W. Christy, *Phys. Rev. B* **21**, 3173 (1980).

³See, for example, P. A. Montano, W. Schulze, B. Tesche, G. K. Shenoy, and T. I. Morrison, *Phys. Rev. B* **30**, 672 (1984); A. Balerna, E. Bernieri, P. Picozzi, A. Reale, S. Santucci, E. Burattini, and S. Mobilio, *ibid.* **31**, 5058 (1985); R. Lamber, S. Wetjen, and N. I. Jaeger, *ibid.* **51**, 10968 (1995), and references therein.

⁴E. Anno, *Surf. Sci.* **260**, 245 (1992).

⁵E. Anno, *Surf. Sci.* **268**, 135 (1992).

⁶E. Anno and T. Yamaguchi, *Phys. Rev. B* **55**, 4783 (1997).

⁷E. Anno and M. Tanimoto, *Phys. Rev. B* **60**, 5009 (1999).

⁸See, for example, E. Anno and R. Hoshino, *J. Phys. Soc. Jpn.* **50**, 1209 (1981).

⁹J. Forssell and B. Persson, *J. Phys. Soc. Jpn.* **29**, 1532 (1970).

¹⁰M. Cardona, *Modulation Spectroscopy* (Academic, New York, 1969), p. 105.

¹¹J. H. Weaver, D. W. Lynch, and C. G. Olson, *Phys. Rev. B* **10**, 501 (1974).

¹²E. Colavita, A. Franciosi, C. Mariani, and R. Rosei, *Phys. Rev. B* **27**, 4684 (1983).

¹³P. Romaniello, P. L. de Boeij, F. Carbone, and D. van der Marel, *Phys. Rev. B* **73**, 075115 (2006).

¹⁴See, for example, A. Kawabata and R. Kubo, *J. Phys. Soc. Jpn.* **21**, 1765 (1966); S. Norrman, T. Andersson, C. G. Granqvist, and O. Hunderi, *Phys. Rev. B* **18**, 674 (1978), and references therein.

¹⁵E. Anno, *J. Appl. Phys.* **104**, 033540 (2008).

¹⁶See, for example, *Optical Properties of Solids*, edited by F. Abelès (North-Holland, Amsterdam, 1972), Chap. 2, Sec. 3.1.

¹⁷See, for example, N. I. Kulikov and E. T. Kulatov, *J. Phys. F: Met. Phys.* **12**, 2267 (1982).

¹⁸See, for example, H. Tups, A. Otto, and K. Syassen, *Phys. Rev. B* **29**, 5458 (1984), and references therein.

¹⁹D. A. Papaconstantopoulos, J. R. Anderson, and J. W. McCaffrey, *Phys. Rev. B* **5**, 1214 (1972).

²⁰N. W. Ashcroft and N. D. Mermin, *Solid State Physics* (Saunders, Philadelphia, 1976), p. 37.

²¹*American Institute of Physics Handbook*, 3rd ed., edited by D. E. Gray (McGraw-Hill, New York, 1972), Sec. 7, p. 6.

²²C. Kittel, *Introduction to Solid State Physics*, 8th ed. (Wiley, New York, 2005), p. 20.

²³B. N. J. Persson, *Surf. Sci.* **281**, 153 (1993), and references therein.